Quantum Electronics **51** (10) 886–893 (2021)

https://doi.org/10.1070/QEL17627

Picosecond hybrid laser based on semiconductor laser, fibre and Nd:YVO_4 amplifiers. Investigation of effects limiting the peak power

I.A. Gorbunov, O.V. Kulagin

Abstract. **Based on a distributed-feedback (DFB) semiconductor laser, an ytterbium fibre amplifier, an Nd:YVO_4 amplifier, and a frequency converter, we designed a hybrid picosecond laser for satellite laser ranging. A gain exceeding 10^8 is achieved while maintaining the temporal shape and spectrum of the pulses, with a low noise level and a divergence close to the diffraction limit. The pulse energy after conversion to the second harmonic at $\lambda = 532$ nm is 2.2 mJ with a duration of 27 ps and a repetition rate of 1 kHz. It is shown that the main effects limiting the peak power are spectrum broadening due to self-phase modulation in a fibre amplifier and large-scale self-focusing in the Nd:YVO_4 amplifier. Optimisation of the amplifier geometry and the use of a uniform profile of the pump radiation intensity make it possible to reduce the effect of self-focusing and increase the energy efficiency of the amplifier.**

Keywords: *picosecond lasers, DFB lasers, fibre amplifiers, large-scale self-focusing.*

1. Introduction

Laser systems that generate picosecond pulses are widely used in materials processing, ranging, nonlinear microscopy, spectroscopy, and biomedical research [1–3]. As a rule, the required pulse durations and peak powers for such applications are achieved using mode-locked lasers characterised by a high pulse repetition rate (tens to hundreds of megahertz), which necessitates their selection. The disadvantages of such lasers are also their rather complicated schemes and the difficulty of external synchronisation of output pulses.

Relatively recently, gain-switched laser diodes (LDs) producing short pulses have appeared [4]. Due to the simple mechanism of pulse generation and the ability to control the pulse repetition rate, they are reliable laser sources for generating nanosecond and picosecond pulses with high pulse-to-pulse stability and very low jitter relative to external sync pulses. This feature allows such LDs to be efficiently synchonised with other systems. Due to the lower pulse energy output than in most solid-state lasers, amplification becomes necessary to achieve the power levels required for many applications. The combination of gain-switched LDs and fibre amplifiers makes it possible to develop a compact and stable source of laser radiation [5–7], which can be widely used. A fibre amplifier provides the necessary amplification as well as high beam quality over a wide range of laser power, while ensuring high efficiency, compactness, reliability, and flexibility in controlling pulse parameters such as repetition rate, shape and duration. For example, in [5–7], the energy of output pulses with a duration of 20–90 ps was 0.3–13 μJ (depending on the aperture of the fibre amplifier) at a repetition rate of 1 MHz or more.

However, for picosecond lasers used in ranging and materials processing, it is necessary to provide higher pulse energy and peak power. In this case, such nonlinear effects as stimulated Raman scattering (SRS) and self-phase modulation, which limit the power of fibre amplifiers, become significant [8]. Recently, lasers have appeared with a semiconductor master oscillator (MO) followed by fibre and solid-state amplifiers, which increase the output radiation energy. However, relatively few publications reporting such lasers are known so far [9–11]. The use of solid-state amplifiers can significantly increase the output pulse energy and average power of these lasers. For example, in [10], the energy of 13-ps output pulses was 0.23 mJ at a repetition rate of 200 kHz and the divergence of the output radiation was close to the diffraction limit. Note also that the width of the output radiation spectrum of picosecond lasers with gain switching and distributed feedback (DFB) lasers is, as a rule, close to the Fourier limit [6, 10]. Therefore, their use as a MO provides a high conversion efficiency of the output radiation frequency, which is important for many applications, including satellite ranging.

This paper presents the results of the development of a picosecond laser with a target set of parameters for satellite ranging. Modern satellite ranging systems require lasers with well-defined values of such characteristics of the output radiation as pulse duration, pulse repetition rate, wavelength and spectrum width [12, 13]. In most of these systems, the pulse repetition rate is 1 kHz or more, and the range measurement accuracy is determined by their duration, which is less than 100 ps. The aim of this work is to design a laser with the hybrid configuration of the scheme presented in the introduction for a satellite laser ranging system at a wavelength of 532 nm with a pulse duration of less than 50 ps, a pulse repetition rate of 1 kHz, and an energy of more than 2 mJ.

2. Experiment

The scheme of the laser developed by us comprises a semiconductor MO, an ytterbium fibre amplifier, a bulk solid-state amplifier based on neodymium-doped yttrium orthovanadate (Nd:YVO_4), and a frequency converter. A schematic of the

I.A. Gorbunov, O.V. Kulagin Institute of Applied Physics, Russian Academy of Sciences, ul. Ulyanova 46, 603950 Nizhny Novgorod, Russia; e-mail: igorbunov@appl.sci-nnov.ru, ok@appl.sci-nnov.ru

Received 27 August 2021
Kvantovaya Elektronika **51** (10) 886–893 (2021)
Translated by V.L. Derbov

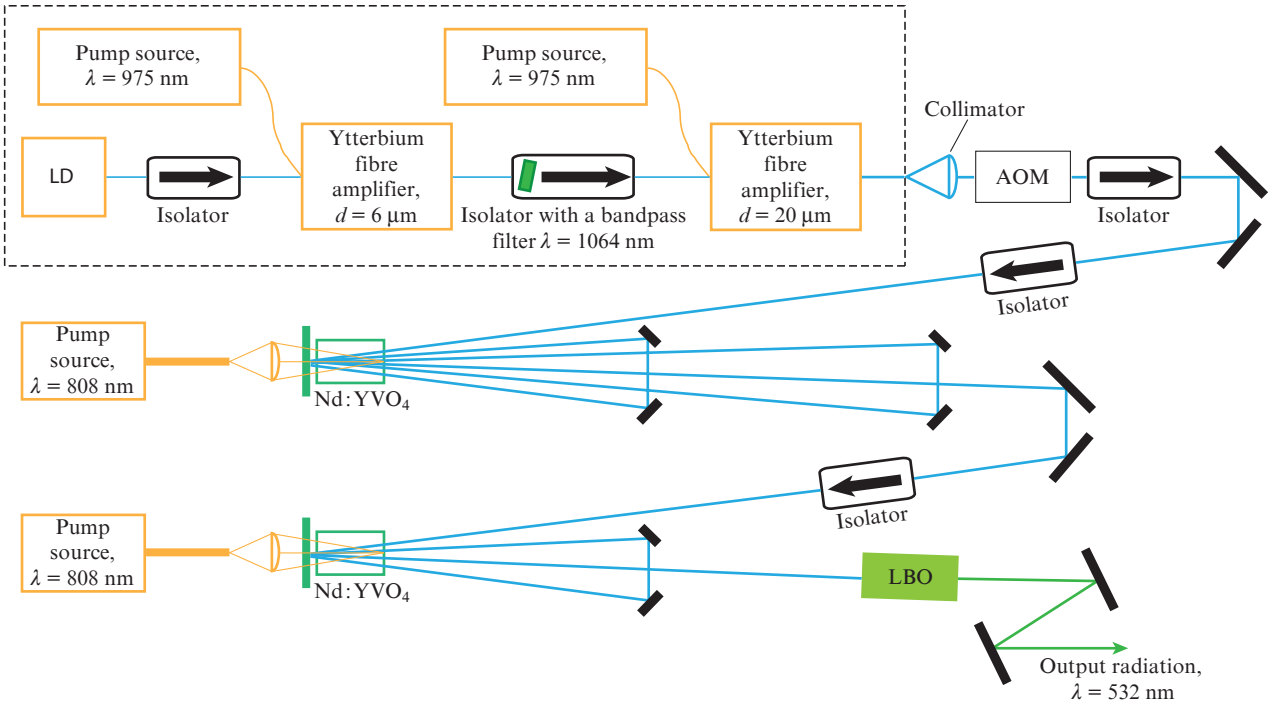

Figure 1. Schematic of the picosecond laser.

picosecond laser is shown in Fig. 1. A semiconductor laser with distributed feedback (DFB) and gain switching, emitting at a wavelength of $\lambda = 1064$ nm, was used as the MO. The MO housing contains a Peltier element that maintains the specified temperature. Thanks to the DFB, it is possible to tune the radiation wavelength in the range 1064.05–1064.85 nm by changing the laser temperature. This allows the wavelength to be tuned to maximise the gain in the neodymium solid-state amplifier. A specially developed driver supplies the LD with short current pulses with a duration of ~1 ns and generates picosecond optical pulses. The maximum pulse repetition rate of the MO is limited by the driver and amounts to 100 kHz, and the average optical pulse power of 1 μW measured in this case corresponds to an energy of 10 pJ in a single pulse. Further work was carried out at a pulse repetition rate of 1 kHz.

The width of the spectrum of the MO pulses, measured with an ASP-150T spectrometer (Avesta-Project LLC), was 0.2 nm at a resolution of 0.1 nm. To achieve the required millijoule level, the pulse energy of a semiconductor laser must be increased by more than 10^8. The MO radiation was coupled out through a single-mode polarisation-maintaining fibre.

The semiconductor MO pulses were amplified in a two-stage fibre amplifier. All used fibre components maintained the polarisation of the radiation. The first stage based on a single-mode ytterbium-doped fibre was pumped by the cw radiation from a single-mode LD at $\lambda = 975$ nm with a power up to 600 mW, propagating along the fibre core 6 μm in diameter. The achieved gain in the first amplifier was ~20 dB. A Faraday isolator with a built-in bandpass filter for $\lambda = 1064$ nm was installed between the amplification stages, which is necessary to suppress amplified spontaneous emission, especially at the maximum of the ytterbium gain line at $\lambda = 1030$ nm. The second ytterbium fibre amplifier based on a fibre with a core diameter of 20 μm and a double cladding was pumped by continuous multimode LD radiation at $\lambda = 975$ nm with a power of up to 9 W. The output radiation of the fibre amplifiers was collimated by an aspherical lens into a beam 1 mm in diameter and directed to bulk amplifiers based on Nd:YVO_4 crystals.

Between the fibre and bulk solid-state amplifiers, two Faraday isolators and an acousto-optic modulator (AOM) with a response time of 100 ns were installed, which deflected part of the radiation at an angle of 1° and suppressed the noise of the fibre amplifiers between amplified pulses. In the absence of AOM, noise amplified in neodymium solid-state amplifiers led to a limitation of the stored energy and a decrease in the gain. After deflection of the pulses by the modulator, their energy was determined from the average radiation power at a pulse repetition rate of 1 kHz, while the spectrometer ASP-150T monitored the radiation spectrum. Initially, the second amplifier used 11 μm fibre, later replaced by 20 μm fibre. This replacement made it possible to reduce the nonlinear spectrum broadening and increase the output pulse energy. Spectrum broadening was caused by the nonlinear effect of self-phase modulation in the fibre when a significant peak pulse power was reached. For a fibre with a core diameter of 20 μm at pulse energies up to 30 nJ, the spectrum did not change after amplification; its width was 0.19 nm. A typical form of the spectrum is shown in Fig. 2a. The minimum change in the spectral width that could be detected with the spectrometer was 0.04 nm. When the energy reached 90 nJ, a noticeable distortion and broadening of the spectrum was already observed (Fig. 2b), which rapidly increased with a further increase in energy. With a significant broadening of the spectrum, the temporal shape of the pulse may be distorted after amplification in relatively narrow-band neodymium amplifiers; therefore, the energy was subsequently limited to a level of 90 nJ, which corresponds to ~3 kW of peak power in the fibre. For comparison, in a fibre with a core 11 μm in diameter at the same energy, a more significant broadening of the spectrum was observed (Fig. 2c).

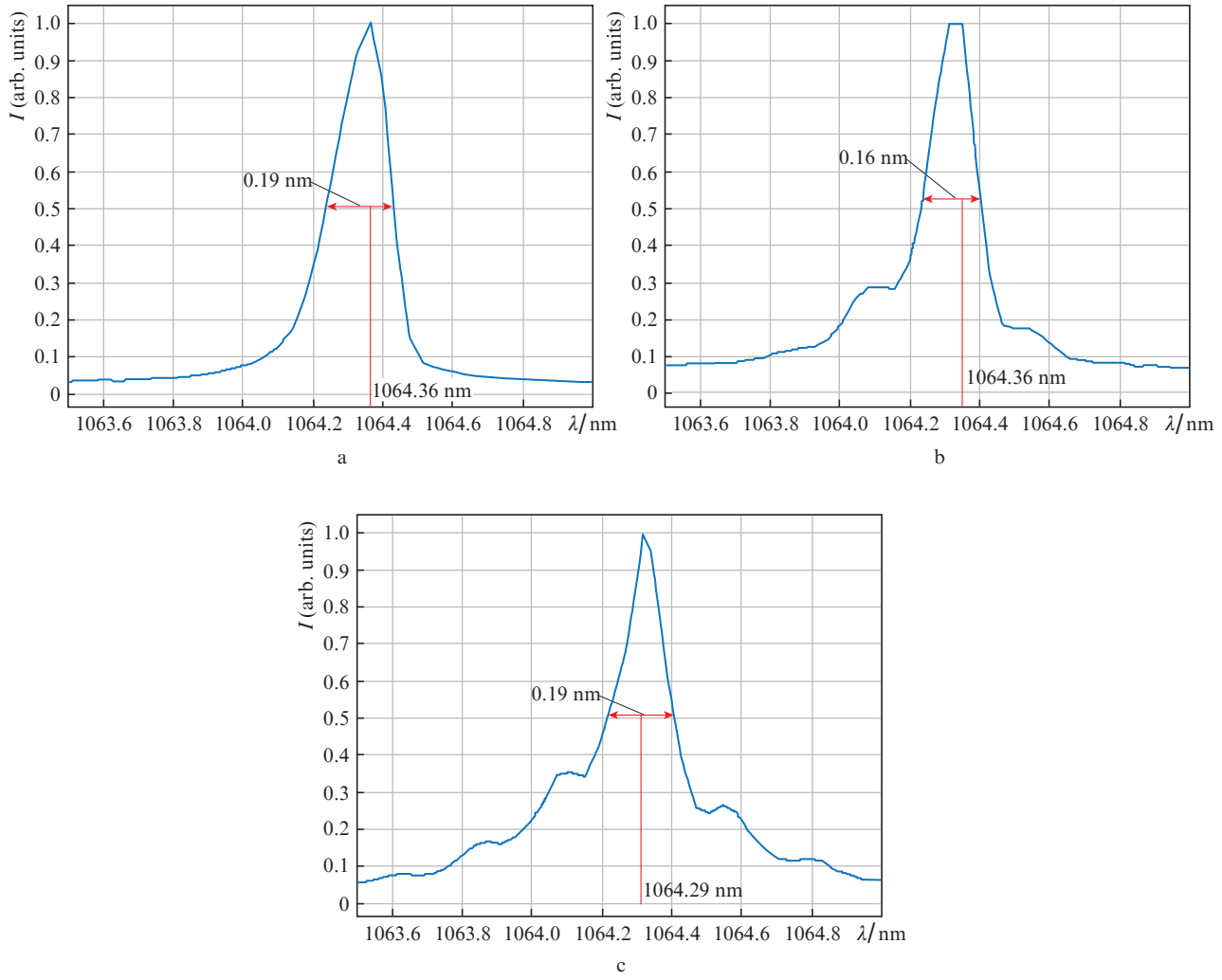

Figure 2. Spectra of laser radiation at the diameters of the fibre amplifier core and pulse energies of (a) 20 μm, 30 nJ, (b) 20 μm, 90 nJ and (c) 11 μm, 90 nJ.

The spectrum broadening is explained by the effect of self-phase modulation (SPM) in optical fibre [8]. Let us consider the propagation through a fibre of a light pulse, described by a field with a normalised amplitude $U(z,T)$ [8] in the absence of group velocity dispersion and absorption. Here z is the longitudinal coordinate in the fibre, and $T = t - z/v_{gr}$ is the time in the coordinate system moving with the group velocity of the pulse v_{gr}. The amplitude $U(L,T)$ at the output of a fibre of length L is determined by the expression [8]

$$U(L,T) = U(0,T)\exp[i\varphi_{nl}(L,T)], \quad (1)$$

where

$$\varphi_{nl}(L,T) = \frac{\omega_0 n_2}{cA_{eff}} LP_0 |\, U(0,T)\,|^2 \quad (2)$$

is the nonlinear phase shift during propagation; P_0 is the pulse peak power; $n_2 = 2.7\times10^{-20}$ m^2 W^{-1} [14] is the nonlinear refractive index of the silica fibre; ω_0 is the centre frequency of the pulsed radiation; A_{eff} is the effective area of the radiation mode in the fibre; and c is the speed of light. For a Gaussian pulse of duration T_0, the field amplitude at the input to the fibre is

$$U(0,T) = \exp\left[-\frac{1}{2}\left(\frac{T}{T_0}\right)^2\right]. \quad (3)$$

Substituting (3) into (2), we find the frequency shift $\delta\omega$ at $z = L$:

$$\delta\omega(T) = -\frac{\partial\varphi_{nl}}{\partial T} = \frac{2T}{T_0^2}\frac{\omega_0 n_2}{cA_{eff}} LP_0 \exp\left[-\left(\frac{T}{T_0}\right)^2\right]. \quad (4)$$

Equating to zero the derivative in expression (4), we find the maximum frequency shift $\delta\omega_{max}$:

$$\delta\omega_{max} = \sqrt{\frac{2}{e}}\frac{1}{T_0}\frac{\omega_0 n_2}{cA_{eff}} LP_0. \quad (5)$$

Let us calculate the frequency shift in the second stage of the fibre amplifier. We assume that the gain is unsaturated; in this case, the peak radiation power increases along the length of the active fibre according to the law $P(z) \sim \exp(\alpha z)$ with the specific gain α. With an active fibre length $L_a = 3$ m and a total gain of 20 dB, $\alpha = 1.54$ m^{-1}. To estimate $\delta\omega_{max}$, instead of LP_0 we substitute in Eqn (5) the result of integrating $P(z)$ over the length of the active fibre $P_{out}L_{eff}$, where P_{out} is the peak power of the pulse at the fibre output; $L_{eff} = \alpha^{-1} =$

0.65 m. The experimentally measured power is P_{out} = 3 kW. The field diameter of the radiation mode declared by the fibre manufacturer is d_m = 15.9 μm. Hence, the effective area of the mode field is

$$A_{eff} = \frac{\pi d_m^2}{4} = 1.99 \times 10^{-10}\ \text{m}^2.$$

For a pulse with a measured duration of 32 ps, the calculated maximum wavelength shift was 0.042 nm, which is close to the measured spectral width. Consequently, in this case, there should already be a noticeable change in it. Note that first, there is a slight decrease in the spectrum width at the centre of the line (Figs 2a, 2b), which may be due to the presence of a negative chirp (frequency modulation) in the initial pulse [8]. Such frequency modulation is typical for gain-switched semiconductor lasers [4].

Another nonlinear effect limiting the peak power in fibre lasers is SRS. We did not observe SRS after amplification of pulses in the developed fibre amplifiers; however, we evaluated the influence of this effect on the amplified radiation with a further increase in the output peak power. The increase in the Stokes radiation power $P_S(z)$ in a laser amplifier of length L_a, caused by SRS, is described by the expression [15] (for stationary SRS, i. e., at pulse durations longer than 1 ps):

$$P_S(L_a) = P_S(0)\exp\left(\int_0^{L_a} gI(z)\,dz\right) = P_S(0)\exp(gI_{out}L_{eff}), \quad (6)$$

where g is the Raman local gain; $I(z) = P(z)/A_{eff}$ is the radiation intensity at the pump wavelength; and $I_{out} = I(L_a)$ is the output intensity. In this case, we neglect the decrease in the intensity of the pump wave during stimulated Raman scattering. The quantity $P_S(0)$ is determined by spontaneous scattering, the power of which is equivalent to one photon per mode (longitudinal or transverse) at the fibre input [15]. For a single-mode fibre and without taking into account the effective narrowing of the SRS gain band

$$P_S(0) = \hbar\omega_S\Delta\nu, \quad (7)$$

where $\Delta\nu$ is the width of the SRS gain spectrum; and ω_S is the frequency of the Stokes radiation. For silica fibre, g = 10^{-13} m W^{-1} at the centre of the line, and $\Delta\nu \approx 7$ THz [16]. For the output power of the pump wave P_{out} = 3 kW, the calculated power of the output Stokes wave $P_S(L_a)$ was only 3.3 μW, and the increment (exponent) in Eqn (6) was 0.98. For such a fibre amplifier, let us estimate the threshold output power at which the Stokes wave power reaches 1% of the pump wave power. From Eqns (6) and (7), the corresponding power P_{th} at the output of the fibre amplifier is determined by the equation

$$\hbar\omega_S\Delta\nu\exp\left(\frac{gP_{th}L_{eff}}{A_{eff}}\right) = 0.01P_{th}, \quad (8)$$

from which we find $P_{th} \approx 61$ kW, the increment being 20. Therefore, SRS is not a limiting factor for the increase in the peak output power of the developed fibre amplifier.

We measured the autocorrelation function (ACF) of pulses at the output of the fibre amplifier using a scanning autocorrelator IRA VISIR (Avesta-Project LLC). By the form of the ACF, the pulse shape is close to Gaussian, although it differs from it near the peak. The pulse duration was calculated based on the ACF (Fig. 3) as 32 ps at half maximum with an error of no more than 10%. Accordingly, the product of the pulse duration and the spectrum width is 1.6, and for a Gaussian transform-limited pulse, it is 0.44.

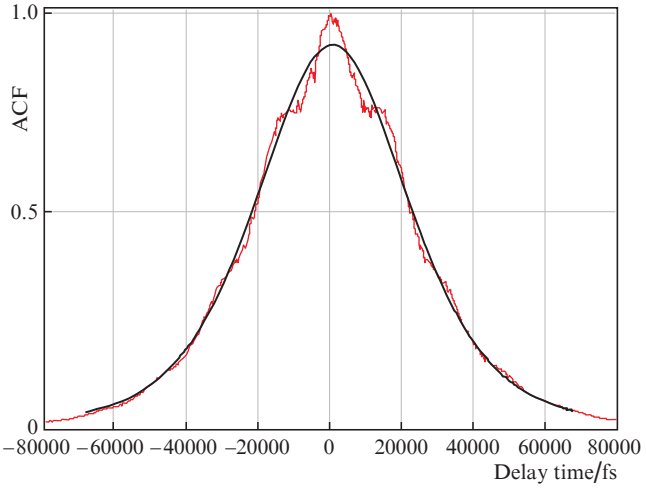

Figure 3. ACF of radiation pulses at a wavelength of 1064 nm after a fibre amplifier and its approximation.

Each of the bulk amplifiers used a square-section active element (AE) made of a Nd : YVO_4 crystal with a neodymium ion concentration of 0.5%, clamped in a copper heat sink. To cool it, a Peltier element was used, which transferred heat to an air-cooled radiator. A dichroic mirror with a high transmittance at a pump wavelength of 808 nm and a high reflectance at λ = 1064 nm was located behind the AE. We used diode pumping with modules having a power of up to 100 W and output to a fibre with a diameter of 400 mm and a numerical aperture of 0.22. The pump radiation emerging from the fibre was focused by an aspherical lens into the AE through a dichroic mirror. In the first amplifier, the AE length was 4 mm, and 85% of the pump radiation was absorbed in it. In the second amplifier, an AE with a length of 5 mm was used. The lifetime of the metastable level in vanadate was approximately 100 μs; therefore, synchronous pumping by pulses with a duration of 100–130 μs was used. The gain cross section in vanadate substantially depends on its temperature [17] and decreases upon heating. In addition, a thermally induced lens appears in the AE; to compensate for it, diverging lenses were installed in front of the amplifiers. Because of these thermal effects, both bulk amplifiers were designed to operate with a certain average heat dissipation rate at a pulse repetition rate of 1 kHz. According to our estimates, the heat dissipation power in each amplifier was 4–5 W.

The first (six-pass) amplifier was optimised to achieve a high gain and a boost pulse energy to submillijoule levels. The diameter of the pump radiation beam in the AE was 1 mm. Pulses with an energy of 60 nJ were amplified to 800 μJ, which corresponds to a gain of 41 dB. With decreasing input energy in the unsaturated regime, a small-signal gain of 48 dB was measured. Further attempts to increase the gain by changing the amplifier parameters led to a rapid increase in amplified spontaneous emission (ASE) even in the absence of a seed. The ASE beam was practically Gaussian and coincided in direction with the picosecond pulse to be amplified. The beam

quality parameter M^2 of the amplified picosecond pulse was measured, which amounted to 1.15. Hereinafter, the M^2 parameter was measured according to the State Standard R ISO 11146-1-2008 method.

The second (four-pass) amplifier was optimised to maximise the extraction of the stored energy and operated in the strong-saturation regime: with a beam diameter of 1.45 mm and a pulse energy of 0.8 mJ at the amplifier input, the energy density was 0.05 J cm^{-2}, which is already close to the saturation energy density of 0.11 J cm^{-2}. For such an amplifier, two fundamental physical limitations are essential: the relatively long lifetime of the lower laser level and the nonlinear effect of large-scale self-focusing. In the geometry used, the time for a picosecond pulse to travel through the AE is less than 100 ps, while the relaxation time of the lower laser level in Nd:YVO_4 is much longer, exceeding 500 ps [18]. In this case, the lower laser level remains populated during the passage of the amplified pulse, which reduces the efficiency of energy extraction [18]. That is why a four-pass scheme was used to increase the energy efficiency of the amplifier. The pump radiation beam had a diameter of 2 mm, pulses with an energy of 0.8 mJ were amplified to 3.1±0.06 mJ (hereinafter, the root-mean-square deviation is given). In the first (six-pass) amplifier, the lifetime of the lower laser level does not affect the gain due to the low pulse energy: with a stored energy of 4 mJ, the fraction of energy extracted from the amplifier is small (no more than 20%). To estimate the noise level, the parameters of the laser noise radiation were measured in the absence of the MO pulse. At a pump energy corresponding to an output energy of 3.1 mJ, the ASE formed a 20 μs pulse with an energy of 0.1 mJ.

The peak power of the pulses at the amplifier output was approximately 100 MW, which was the reason for the appearance of large-scale self-focusing in the AE material. At the entrance to the second (four-pass) amplifier, the beam was close to Gaussian, but at the exit a significant distortion of the profile and narrowing of the beam were observed when the output energy reached 2–3 mJ. Generally speaking, several factors could lead to the beam distortion: inhomogeneous transverse profile of the pump bema and hence nonuniform amplification profile, spherical aberration of the thermal lens in the AE, and self-focusing. It is shown below that nonlinear focusing leads to narrowing of the beam, as well as to optical breakdown in subsequent optical elements, to a decrease in the energy efficiency of the amplifier, and to a deterioration in the beam quality parameter. Self-focusing developed when the beam passed through the terbium-gallium garnet (TGG) crystal of the Faraday rotator before the second amplifier and through the second Nd:YVO_4 amplifier. Let us estimate the B-integral when a Gaussian beam of pulsed laser radiation passes through these elements using the formula [19]

$$B = \frac{2\pi}{\lambda}\int n_2 I(z)\,\mathrm{d}z\,. \tag{9}$$

Table 1 presents its calculated values for the passage of beams with measured parameters through TGG and Nd:YVO_4 elements. The peculiarity of the amplifier geometry is that the dichroic mirror reflecting the amplified radiation is located close to the AE (see Fig. 1); therefore, in calculation of B, two successive passes of AEs with a length of 5 mm were considered one pass of an element 10 mm long. The two different calculations of B for Nd:YVO_4 in Table 1 correspond to the first and second pairs of passes through the amplifier. The sum of B-integrals is approximately 1.5; therefore, a further increase in the pulse energy can also lead to a small-scale self-focusing.

Table 1. Calculated values of the B-integral when the pulse passes through the laser elements. The used parameters of the elements and the radiation pulse are given.

Element	n_2 /10^{-15} cm^2 W^{-1}	Length /mm	Average energy /mJ	Beam diameter /mm	B-integral
TGG	1.72 [20]	20	0.7	1.45	0.54
Nd:YVO_4	1.26 [21]	10	1.4	1.45	0.4
Nd:YVO_4	1.26 [21]	10	2.6	1.7	0.53

In the experiment, to confirm the effect of self-focusing, we reduced the pulse energy before the Faraday rotator and the second amplifier from 0.7 to 0.1 mJ. In this case, after four passes through the amplifier, the output energy decreased from 2.7 to 1.6 mJ, and the effect of large-scale self-focusing became much smaller. The output beam was measured with an Ophir SP-620U camera at a distance of 16 cm from the output end of the amplifier. For comparison with experiment, the profiles of the output beam were also calculated taking into account the nonlinear phase shift when passing through the above-described laser elements. The initial beam was considered Gaussian with a diameter of 1.45 mm (at the e^{-2} intensity level) with a plane wavefront before the TGG crystal. Each element was considered a flat phase screen, for which the nonlinear phase shift was calculated

$$\varphi_{\mathrm{nl}}(r) = \frac{2\pi}{\lambda} n_2 I(r) L_{\mathrm{nl}}, \tag{10}$$

where $I(r)$ is the intensity averaged over the length of the nonlinear element; L_{nl} is the distance of propagation in it; and r is the radial coordinate in the beam. Similarly to Table 1, the first element was a TGG crystal, the second was a double-length Nd:YVO_4 crystal (1st and 2nd passes), and the third was another double-length Nd:YVO_4 crystal (3rd and 4th passes). For an input pulse with an energy of 0.1 mJ, the average energies during the passage of these elements were 0.1, 0.35, and 1.05 mJ, respectively, and for a pulse with an energy of 0.7 mJ they were 0.7, 1.4, and 2.4 mJ, respectively. Changes in the amplitude and phase of the light wave field during the propagation of the beam in free space between the elements were found from the solution of the wave equation in the quasi-optics approximation [22], and the change in the beam profile during amplification was not taken into account. The profiles measured and calculated with and without nonlinearity of the optical elements are shown in Fig. 4. In Fig. 4a, at an output energy of 1.6 mJ, the self-focusing effect is weakly pronounced. In Fig. 4b, at an output energy of 2.7 mJ, a noticeable narrowing of the beam is observed, which is described well by taking into account large-scale self-focusing in the calculation.

We investigated the possibilities of maximising the energy extraction in a four-pass amplifier under nonlinear focusing conditions while maintaining the beam quality and in the absence of optical breakdown. To this end, the diameter of the amplified beam and the diameter and profile of the pump radiation beam were optimised. Observation of the AE image by the camera allowed us to measure the luminescence intensity profile at a wavelength of 1064 nm, which coincides with the pump radiation intensity profile. Figures 5a and 5b show the recorded two-dimensional distributions of the lumines-

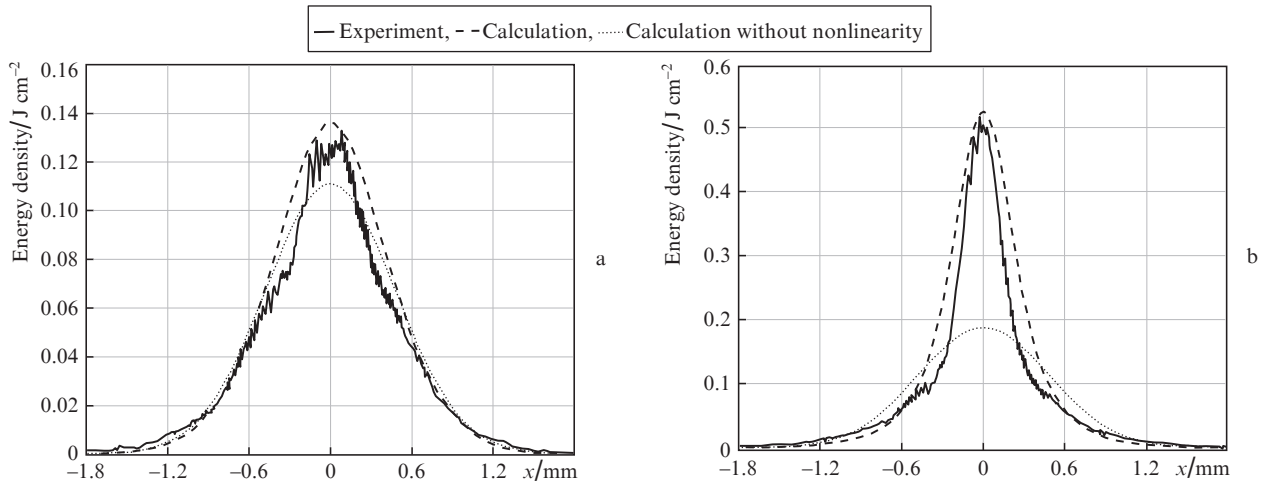

Figure 4. Measured and calculated transverse beam profiles at the output of the second amplifier for output pulse energies of (a) 1.6 and (b) 2.7 mJ.

cence intensity and distribution profiles along two transverse axes, in which the square aperture of the AE is visible. Figures 5c and 5d present the intensity distributions and profiles of the output beam at a distance of 160 mm from the amplifier. For the profile of the pump radiation intensity in Fig. 5a, which is close to Gaussian, a pronounced nonlinear focusing

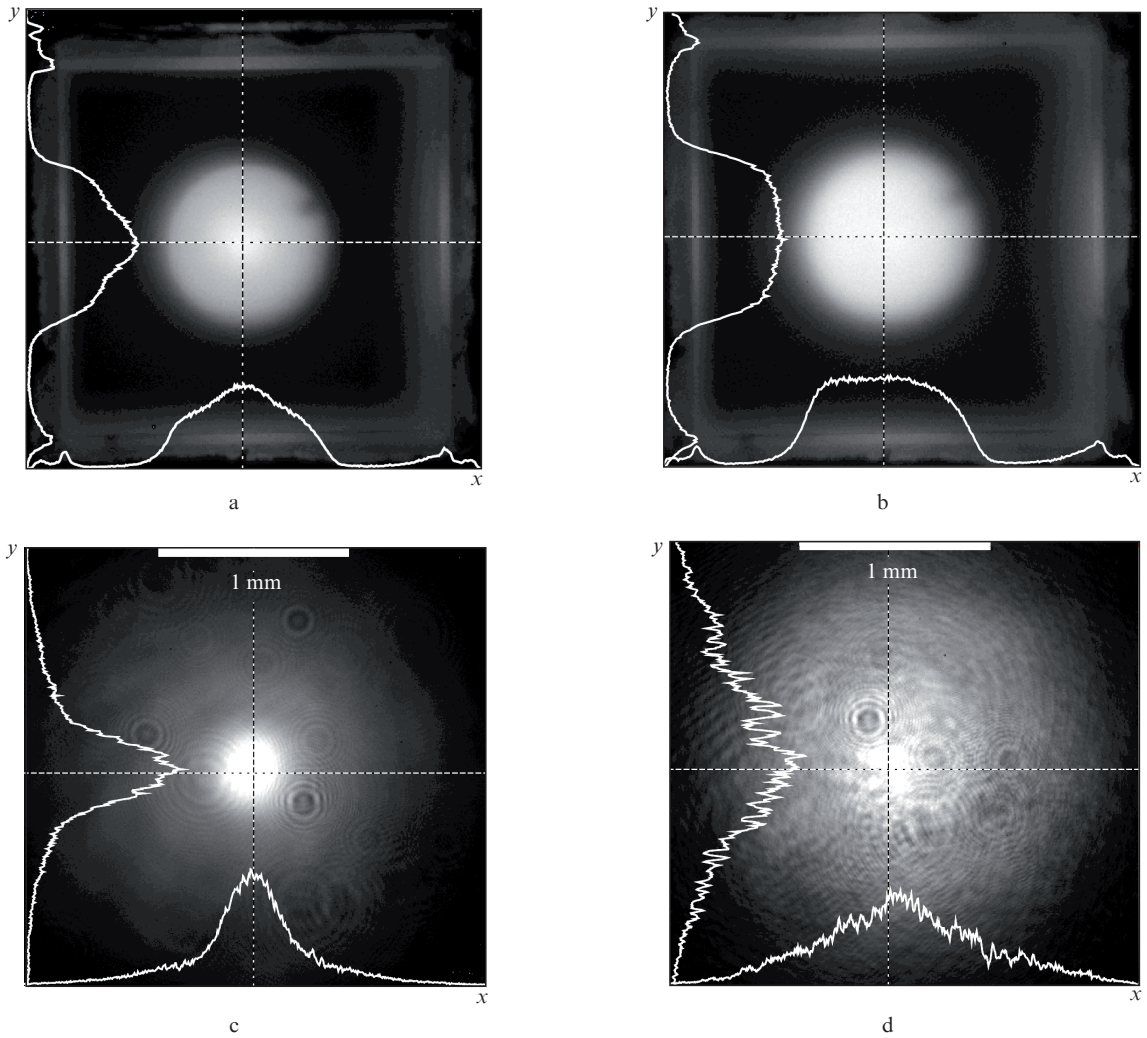

Figure 5. (a, b) Luminescence intensity profiles in the amplifier and (c, d) corresponding intensity profiles of amplified radiation beams.

of the beam is observed (Fig. 5c). At the same time, with a super-Gaussian, close to a top-hat profile of the pump intensity in Fig. 5b, the self-focusing in the output beam in Fig. 5d significantly decreases. As a result of minimising this effect, the energy efficiency of the amplifier increases – the output pulse energy increases from 2.7 to 3.1 mJ. In addition, the quality of the beam improves: the measured quality parameter $M^2 = 1.65$ for the output beam in Fig. 5d and 1.86 for the beam in Fig. 5c. In this case, the output amplified beam also has a super-Gaussian profile immediately after the AE.

To convert the output radiation to the second harmonic, an LBO crystal was used, placed in a thermostat with a temperature of about 40 °C, with type-I phase matching. The conversion efficiency was more than 70%, while radiation pulses at a wavelength of 532 nm had an energy of 2.2±0.07 mJ. The achieved high efficiency confirms the absence of a significant admixture of noise emission at a wavelength of 1064 nm. The beam divergence was close to the diffraction limit with $M^2 = 1.5$. The duration of radiation pulses at a wavelength of 532 nm, determined from the measured ACF, was 27 ps (Fig. 6b). The measured spectrum of output pulses with a width of 0.11 nm is shown in Fig. 6, but taking into account the fact that the instrumental function of the spectrometer was 0.1 nm, the real width of the spectrum may be smaller. The width and position of the spectral maximum were stable from pulse to pulse.

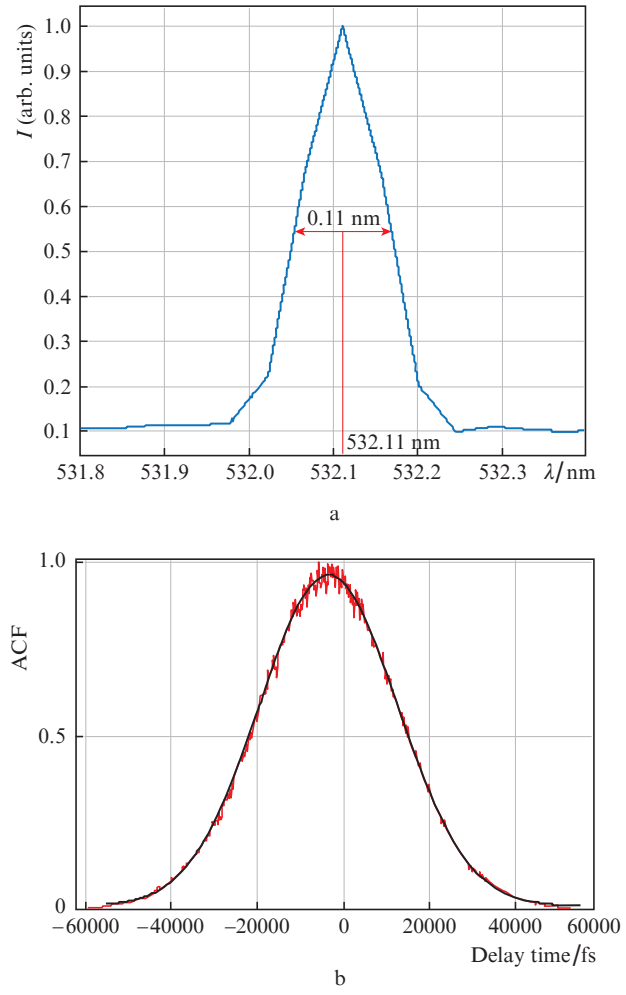

Figure 6. (a) Spectrum of laser pulses and (b) ACF after conversion to the second harmonic.

3. Conclusions

In the course of the work, a hybrid picosecond laser for satellite laser ranging was developed, based on a semiconductor MO, a fibre amplifier, a bulk solid-state amplifier, and a frequency converter. Amplification of the MO pulses exceeding 10^8 was achieved, with stable temporal shape and spectrum, a low noise level, and a near-diffraction-limited beam. The output pulse energy at a wavelength of 1064 nm was 3.1± 0.06 mJ with a duration of 32 ps, and after conversion to the second harmonic with λ = 532 nm it was 2.2± 0.07 mJ with a duration of 27 ps; the repetition rate was 1 kHz. The achieved pulse energy and peak power are the highest we know for lasers of this type. The physical limitations of the peak power during amplification of picosecond pulses in fibre and bulk amplifiers are analysed. It is shown that the main limiting factors are spectrum broadening due to SPM in a fibre amplifier and large-scale self-focusing in elements of bulk amplifiers. Optimisation of the amplifier geometry and the use of a uniform profile of the pump radiation intensity made it possible to reduce self-focusing and increase the energy efficiency of the amplifier.

Acknowledgements. The work was performed within the framework of the scientific and technical programme 'Technologia-SG' of the Union State and was supported by the Ministry of Science and Higher Education of the Russian Federation (State Task of the IAP RAS, Project No. 0035-2019-0012).

References

1. Phillips K.C., Gandhi H.H., Mazur E., Sundaram S.K. *Adv. Opt. Photon.*, **7**, 684 (2015).
2. Erdmann R., Langkopf M., Lauritsen K., Bulter A., Wahl M., Wabnitz H., Liebert A., Moller M., Schmitt T. *Proc. SPIE*, **5693** 43 (2005).
3. Müller A., Marschall S., Jensen O.B., Fricke J., Wenzel H., Sumpf B., Andersen P.E. *Laser Photonics Rev.*, **7**, 605 (2013).
4. Pataca D.M., Gunning P., Rocha M.L., Lucek J.K., Kashyap R., Smith K., Moodie D.G., Davey R.P., Souza R.F., Siddiquir A.S. *J. Microwav. Optoelectron.*, **1**, 46 (1997).
5. Kanzemeyer S., Sayinc H., Theeg T., Frede M., Neumann J., Kracht D. *Opt. Express*, **19**, 1854 (2011).
6. Dupriez P., Piper A., Malinowski A., Sahu J.K., Ibsen M., Thomsen B.C., Jeong Y., Hickey L.M.B., Zervas M.N., Nilsson J., Richardson D.J. *IEEE Photonics Technol. Lett.*, **18**, 1013 (2006).
7. Liu H., Gao C., Tao J., Zhao W., Wang Y. *Opt. Express*, **16**, 7888 (2008).
8. Agrawal G.P. *Nonlinear Fiber Optics* (New York: Academic Press, 2001).
9. Ueda K., Orii Y., Takahashi Y., Okada G., Mori Y., Yoshimura M. *Opt. Express*, **24**, 30465 (2016).
10. Kohno K., Orii Y., Sawada H., Okuyama D., Shibuya K., Shimizu S., Yoshimura M., Mori Y., Nishimae J., Okada G. *Opt. Lett.*, **45**, 2351 (2020).
11. Kurita T., Kawai K., Morita T., Iguchi T., Kato Y. *OSA Continuum*, **3**, 1711 (2020).
12. Sadovnikov M.A., Shargorodskiy V.D. *Proc. 19th International Workshop on Laser Ranging* (Annapolis, USA, 2014) p. 3025.
13. Vasiliev V.P. *Phys. Usp.*, **61**, 707 (2018) [*Usp. Fiz. Nauk*, **188**, 790 (2018)].
14. Milam D., Weber M.J. *J. Appl. Phys.*, **47**, 2497 (1976).
15. Smith R.G. *Appl. Opt.*, **11**, 2489 (1972).
16. Stolen R.H., Ippen E.P. *Appl. Phys. Lett.*, **22**, 276 (1973).
17. Delen X., Balembois F., Georges P. *J. Opt. Soc. Am. B*, **28**, 972 (2011).
18. Bibeau C., Payne S.A., Powell H.T. *J. Opt. Soc. Am. B*, **12**, 1981 (1995).

19. Mak A.A., Soms L.N., Fromzel V.A., Yashin V.E. *Lazery na neodimovom stekle* (Neodymium Glass Lasers) (Moscow: Nauka, 1990) p. 246.
20. www.northropgrumman.com/space/synoptics-products-faraday-crystals/.
21. Vodchits A.I., Orlovich V.A., Apanasevich P.A. *J. Appl. Spectrosc.*, **78**, 918 (2012).
22. Akhmanov S.A., Nikitin S.Yu. *Physical Optics* (Oxford: Clarendon Press, 1997; Moscow: Nauka, 2004).